Generation of controlled radiation sources in the atmosphere using a dual femtosecond /nanosecond laser pulse

Z. Henis,[1,a)] G. Milikh,[1] K. Papadopoulos,[1,2] and A. Zigler[2,3]
[1]*Department of Astronomy, University of Maryland, College Park, Maryland 20742, USA*
[2]*BAE SYSTEMS, Washington DC 20037, USA*
[3]*Racah Institute of Physics, Hebrew University, Jerusalem 91904, Israel*

(Received 24 December 2007; accepted 17 March 2008; published online 23 May 2008)

The generation of powerful radiation sources at predetermined remote locations in the atmosphere using dual femtosecond/nanosecond laser pulses is proposed. The plasma channel generated in the wake of the collapsed beam formed during intense ultrashort pulse propagation in the atmosphere serves as seed target plasma to absorb energy delivered by a long pulse laser, inducing further ionization and significantly enhancing the energy density locally deposited in the plasma. Energy equipartition on time scales shorter than 1 μs results in large energy density in the heated air and is followed by several orders of magnitude enhancement of the radiation emitted by the plasma channel. The effect is demonstrated using a one-dimensional computational study. A proof-of-principle experiment is suggested. © *2008 American Institute of Physics*.
[DOI: 10.1063/1.2927457]

I. INTRODUCTION

Recent experimental results indicate that ultrashort powerful lasers (USPL), such as Ti:sapphire femtosecond lasers, can propagate over distances of several tens of kilometers, collapse and form narrow light filaments at distances from several tens to several hundreds on meters in air (see Ref. 1 for a recent review). This phenomenon opens up the potential of using the plasma created in the wake of these filaments to generate remotely radiation sources with controlled emission characteristics. Such radiating sources in air are relevant to a number of applications in the areas of active and passive remote sensing.

In assessing this possibility, we note that long range propagation followed by filamentation in air requires laser power in excess of the threshold for filamentation instability.[2] Following the beam collapse single or multiple filaments are formed that are observed to propagate over distances from several tens to several hundreds of meters. The propagation mode is the result of a dynamic equilibrium among beam Kerr self-focusing, diffraction, and defocusing caused by the laser induced multiphoton ionization. In the wake of the self-guided pulse, a plasma column is created with electron number density of $10^{16}-10^{17}$ cm^{-3}, over a distance that depends on the initial laser intensity, wavelength, and local air pressure. This length may be of the order of few meters. Several filaments are formed for laser power higher than the self-focusing threshold. The filaments have a typical diameter of about 100 μm, and contain a high, quasiconstant laser intensity of about 10^{14} W/cm^2, which leads to self-phase modulation and generation of a broadband white light continuum from the ultraviolet (UV) to the midinfrared (IR). About 10%–20% of the total pulse energy (usually of the order of few millijoules) is localized in the filaments, while the rest of the energy remains in the surrounding unfocused beam. The filaments generated by the USPL are nonequilibrium plasma, i.e., electrons with temperature approaching 1 eV, cold ions, and ambient gas. The lifetime of these plasma filaments is limited to hundreds of nanosecond by recombination and attachment of electrons to oxygen molecules. The resultant radiating energy per pulse is relatively low for practical applications. Moreover, energy radiated by the filaments cannot be increased by increasing the USPL energy because of the mechanism of filament generation.[1]

The objective of this paper is to demonstrate that by complementing the subpicosecond USPL with a long pulse laser (LPL), such as a carbon dioxide (CO_2) laser, with submicrosecond pulse duration and several tens of joules energy/per pulse, it is possible to extend the lifetime of the originally USPL generated plasma to millisecond time scale, and thus generate radiating plasma sources with controlled spectral characteristics at predetermined remote locations, with radiating energy per pulse, exceeding the one resultant from the use of only a USPL by more than four orders of magnitude. The role of the LPL is to increase the electron density and temperature at the location of the USLP generated plasma thereby reducing the time of energy equipartition with the neutrals. The increase in the local energy density of the neutral gas leads to the enhancement of the radiation energy emitted by the channel. Notice that the idea of using a laser pulse to delay the decay of plasma channels in air by detaching electrons from oxygen molecules was previously suggested, in the context of triggering and guiding of lightning discharges.[5,6]

In the dual laser pulse (DLP) approach proposed here the USPL is delivered to a desired location, where it collapses with intensity that exceeds the threshold for multiphoton ionization, resulting in the formation of a plasma channel with density and size such that it can interact and absorb efficiently the energy of the LPL, by inverse bremsstrahlung over short distance. The initial plasma generated by the

a)Electronic mail: zoharhenis@gmail.com.

USPL provides seed electrons for collisional breakdown and heating by the LPL pulse. The CO_2 laser contains sufficient energy to maintain the plasma and increase its energy density. Due to its long wavelength, the CO_2 laser is highly absorbed by the plasma channel. At characteristic channel electron density of the order of 10^{17} cm^{-3}, 95% of the CO_2 laser is absorbed in a length of 1 cm. The long wavelength and the long time duration of the CO_2 laser result in significant electron heating and increase of the plasma density by collisional ionization. This results in decrease of the absorption length and equipartition time followed by significant increase in the energy density of the neutrals. As a consequence of the CO_2 induced laser heating and of the associated increase in the local energy density, the energy radiated by the plasma increases by several orders of magnitude. Furthermore, its spectral distribution can be controlled by the intensity of the CO_2 laser. This dual-pulse laser configuration enables the generation of a remote and powerful radiation source, a plasma flare, in the atmosphere.

Notice that, for applications requiring propagation of femtosecond laser pulses in the atmosphere, it is important to control the onset of filamentation at ranges from hundreds of meters up to several kilometers. This control can be achieved by launching negatively chirped laser pulses.[2] Short, high power laser pulses propagating vertically in the atmosphere over more than 20 km have been observed.[3] Furthermore, a new technique to control the filamentation distance based on the use of a double-lens telescopic system was recently developed.[4]

Section II of the paper analyzes the interaction of the DLP with air and describes the temporal evolution of the plasma parameters, based on a fluid code. Molecular excitation and the associated emission are discussed in Sec. III.

II. A COMPUTATIONAL STUDY OF DLP REMOTE GENERATION OF RADIATION SOURCES

A computational study was performed using a one-dimensional (1D) model that describes the simultaneous interaction of the two laser pulses with air. The model includes multiphoton and impact ionization, recombination, attachment, detachment and dissociation, electron Joule heating, hydrodynamic, and shock phenomena. The electrons are heated by inverse bremsstrahlung and cooled by transferring energy to the air molecules and by expansion. The hot electrons ionize, excite, and dissociate air molecules. The air is heated due to the energy transfer from the electrons through electronic and vibrational excitations of molecules, and cooled by expansion and by heat flow at the plasma boundary. The channel is modeled by a cylinder with time dependent radius $R(t)$. A 1D expansion in the radial direction only is considered. This is justified by the fact that the length of plasma created by the short pulse laser is much longer than its radius. The radial expansion of the hot plasma generates a shock wave in the ambient air, which decelerates the expansion.

The additional ionization and electron heating generated by the long pulse CO_2 laser is accompanied by heating of the neutrals and excitation of molecules and atoms by electron impact, followed by broadband emission from UV to mid-IR. Ionization and excitation rates averaged over a Maxwellian electron energy distribution function were used.[9–12] The following 20 species of the air plasma are considered in the model: ground states of air molecules O_2, N_2, CO_2, excited states of molecules, $N_2(A)$, $N_2(B)$, $N_2(C)$, $N_2(a')$, $O_2(a)$, $O_2(b)$, $CO_2(001)$, O and N atoms, electrons, positive ions, O_2^+, N_2^+, O^+ in ground state, $N_2^+(B)$, and negative ions O_2^-, O^-, in addition we consider vibrationally excited N_2. The reactions among these species include multiphoton and impact ionization, two-body and three-body recombination, dissociation, excitation, attachment, detachment, decay by molecular collisions, and radiative decay.[8] The code follows separately the evolution of the electron temperature T_e and a single air temperature T_{air}, assigned to all molecules, atoms, and ions, justified by their fast energy equilibration time, stemming from their similar mass. It is assumed that the density and the temperature of these species in the cylinder is uniform, implying a common radial velocity v for all the species, varying linearly as a function of the radial coordinate from $v(r=0)=0$ to $v(r=R)=\dot{R}$. Losses by thermal conduction at the plasma boundary are included by approximating the heat flux, $\kappa\nabla T \sim 2d\chi c_{v,air}(T_{air}-T_s)/R$, where $\chi=0.15$ cm^2/s is the thermal diffusivity of air at standard conditions,[7] T_s is the temperature of the shock generated in air by the expansion of the plasma channel, and $d=2$ is a parameter accounting for other mechanisms for heat dissipation, such as ambipolar diffusion.[9] In the framework of the model, the plasma channel evolution is obtained by solving 24 coupled first order differential equations in time, for the 20 number densities of the species listed above, the electron and air temperatures, the channel radius, and expansion velocity.

TABLE I. Laser pulse parameters used in the simulation.

	Intensity (W/cm^2)	Pulse duration (s)	Wavelength (μm)
Short pulse	8×10^{13}	10^{-13}	0.8
Long pulse	6×10^{6}	10^{-7}	10.6

The system evolution was examined separately for irradiation with a USPL laser only and for the DLP case, assuming a plasma radius of 100 μm, of the order of the size of filaments observed in experiments.[1] The laser parameters used in the calculations are listed in Table I. These parameters are indicative of USPL intensity in a single filament and realistic CO_2 laser intensities that can be achieved after propagation of the order of 1 km.

Figure 1 shows the temporal evolution of the charged particles for the case of a plasma channel generated with a short intense laser pulse only. The electron density increases sharply during the laser pulse mainly due to multiphoton ionization of O_2 molecules and reaches a maximum at 1.1×10^{17} cm^{-3}, and then decreases due to recombination and attachment. The electron density decays by few orders of magnitude after hundreds of nanoseconds. The temporal evolution of electron and the air temperatures are shown in Fig. 2. The electron temperature increases sharply to a maximum of about 0.85 eV during the laser pulse and then decreases to

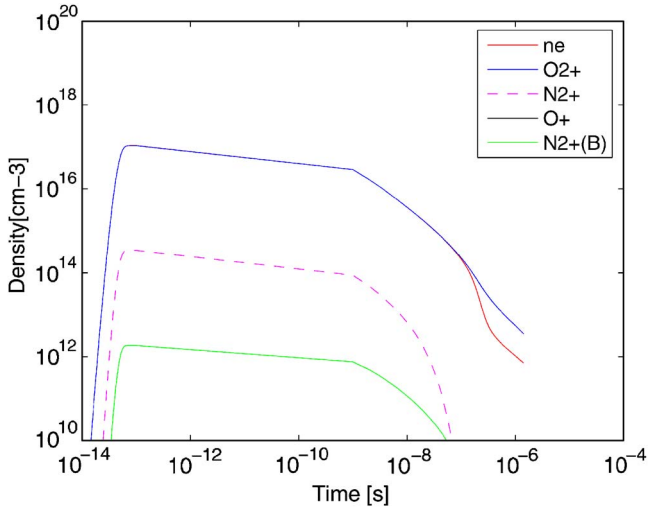

FIG. 1. (Color online) Temporal evolution charged particle number densities for USPL illumination.

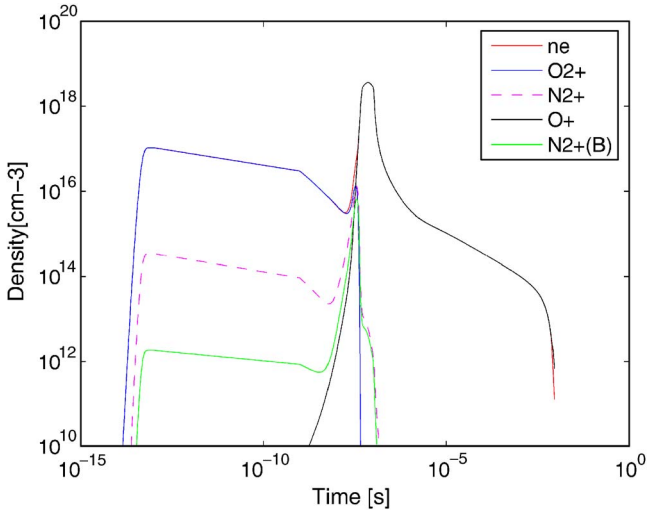

FIG. 3. (Color online) Temporal evolution of charged particle number densities for DLP case.

the ambient temperature after about 1 μs that corresponds to the relaxation time for energy equipartition between the electron neutral gas, that for air and in practical units is given by $\tau \approx (3\times 10^{19}/N)(eV/T_e)$ μs. Following this the neutral gas and electron temperatures equilibrate at a common temperature given by $T \approx T_0 + (n_e/N)T_{e0}$, where T_{e0} and n_e are the electron temperature and density at the end of the USPL and T_0 the ambient gas temperature. For the values shown in Figs. 1 and 2, the change of the gas temperature is less than 3×10^{-2} eV. Namely, the energy density absorbed by the electrons ($\approx$0.01 J/cm^3) from the USPL is not sufficient to increase the air temperature to any extent. As a result, the air remains cold and its radiation properties are extremely limited.

Figure 3 displays the evolution of the number densities of the charged particles as a function of time for DLP case. The electron density increases sharply during the short pulse, followed by a further increase due to the absorption of the CO_2 laser. By the end of the long pulse laser, the electron temperature reaches approximately 5 eV and the electron density a maximum value of 4×10^{18} cm^{-3}, due to impact ionization mainly of O, generated by the electron impact dissociation and recombination of O_2^-. The number densities of the negative ions O_2^- and O^- decrease during the second pulse irradiation, as detachment dominates attachment at the high temperature resulting from the plasma heating. The number density of O_2 and N_2 molecules and atomic O and N as function of time are shown in Fig. 4. The density of O_2 and N_2 decreases due to dissociation and ionization, then a recurrence occurs, as three-body recombination takes place.

The most important effect is shown in Fig. 5, indicating that following the termination of the long pulse and on the energy equipartition time τ, that in this case is a fraction a microsecond, the common temperature T of the electron and neutral gas is approximately 0.7 eV. This is consistent with $T \approx T_0 + (n_e/N)T_{e0}$, but with $n_{e0} \approx 4\times 10^{18}$ cm^{-3} and $T_{e0} \approx 5$ eV. Namely, the electron density increase led to a much shorter laser absorption length resulting in a significant increase of the energy density absorbed by the electrons ($\approx$20 J/cm^3) and quickly shared with the neutral gas. For

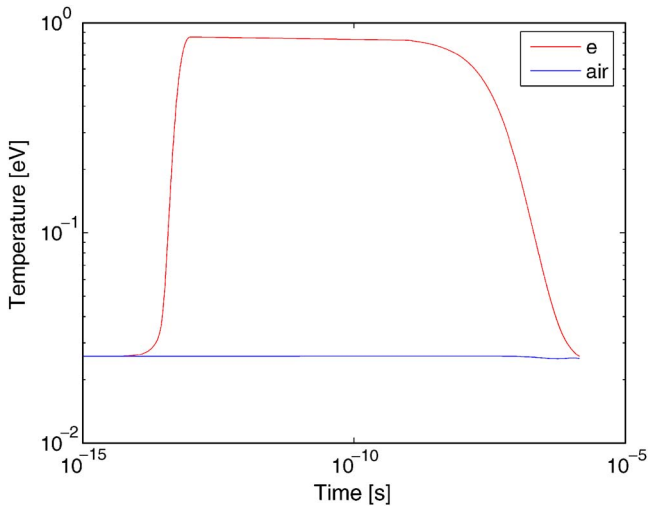

FIG. 2. (Color online) Temporal evolution of electron and air temperatures for USPL illumination.

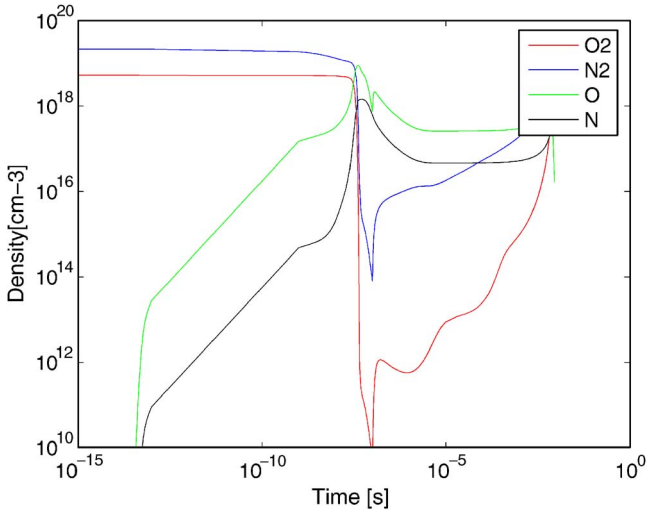

FIG. 4. (Color online) Temporal evolution of neutral species number densities for DLP case.

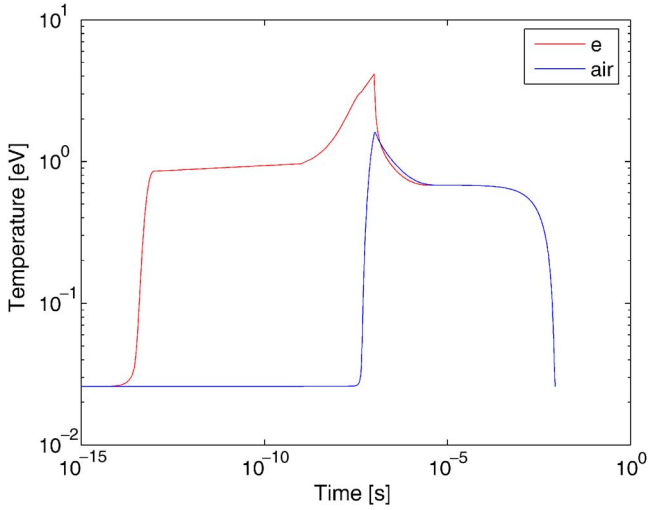

FIG. 5. (Color online) Temporal evolution of electron and air temperatures for DLP case.

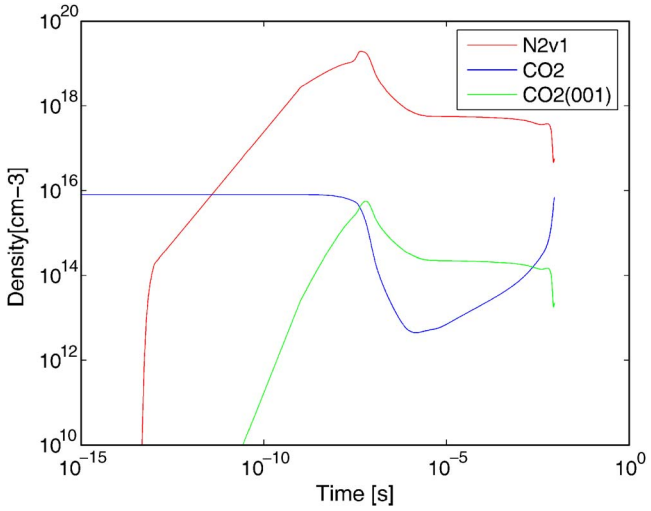

FIG. 7. (Color online) Temporal evolution of the number densities of the species $N_2(v=1)$, CO_2, and $CO_2(001)$ for DLP case.

times longer than the CO_2 pulse duration, the air cools due to expansion and thermal conduction, reaching the ambient temperature after about 10 ms. This is of the order of the characteristic for heat conduction time R^2/χ_h.

The plasma channel radius as a function of time is shown in Fig. 6. The hot plasma starts expanding after about 10^{-7} s, of the order of the characteristic time of hydrodynamic expansion $t_h \sim R/\sqrt{k_B T_{\text{air}}/m_{\text{air}}}$. The plasma radius increases to about 600 μm and then decreases, due to the shock pressure and cooling.

III. PLASMA EMISSION ESTIMATES

Detailed estimates of the plasma emission including propagation of the emitted radiation from the plasma to the detector are currently in progress and will be published later. We restrict our analysis below to approximate estimates of the spectral emission from the plasma flare, predominantly to indicate its high efficiency and control of the gross spectral properties.

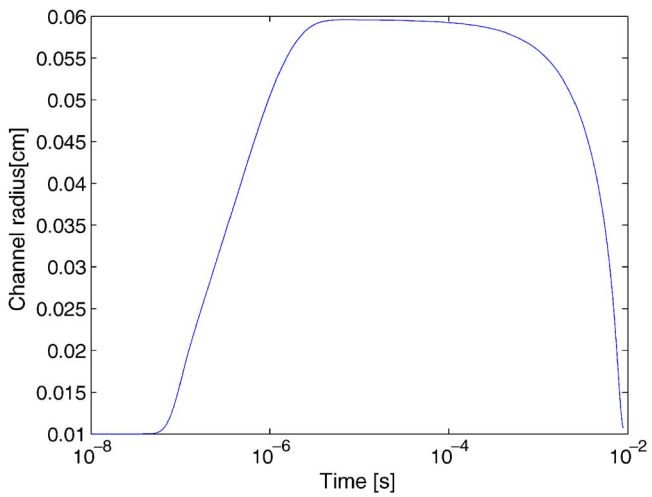

FIG. 6. (Color online) Temporal evolution of the plasma channel radius for DLP case.

Spectroscopic studies of short pulse laser produced plasmas in air indicate that the radiation emitted is mainly in the visible range due to excited molecular nitrogen bands,[13,14] such as the second positive band of N_2 and the first negative band of N_2^+. Continuum emission was observed to dominate plasmas produced by continuous CO_2 lasers,[15] while plasmas generated by pulsed CO_2 lasers excite mostly atomic nitrogen and oxygen lines.[16] In order to demonstrate the capabilities of the DLP approach as radiation source, we confine ourselves here to infrared and visible radiation. The estimates of the emission from excited CO_2 molecules (4.26 μm), the first positive band of N_2 (1.046 μm), the second positive band of N_2 (0.337 μm), and the first negative band of N_2^+ (0.391 μm) are based on the computational results presented in Sect. II. The above wavelengths associated with each molecular band correspond to the center of the band.

The infrared emission at 4.26 μm is the result of direct excitation of the N_2 vibrational levels by direct electron impact, followed by resonant transition of nitrogen vibrons to the CO_2 vibrational level, whose lifetime is much shorter than that of nitrogen. Subsequently, the volumetric emission at 4.26 μm is calculated from the time dependent population of the CO_2 (001) $n_{\text{CO}_2(001)}$ shown in Fig. 7, using the formula $W_{4.26\mu m}(J/\text{cm}^3) = h\omega/\tau \int_0^{t_c} dt \cdot n_{\text{CO}_2(001)}$ and taking into account competing processes, such as de-excitation of the N_2 vibrational level by collisions with oxygen.[12] In the volumetric emission formula, $\tau = 2.5$ ms is the lifetime of CO_2 (001) level, $h\omega = 0.29$ eV its energy, and t_c is the cooling time of the plasma to ambient temperature. As seen in Fig. 7, more than 50% of the nitrogen molecules are vibrationally excited during the long laser pulse, leading to a similar excitation fraction of the CO_2 molecules. After the pulse termination the population of the excited CO_2 molecules decreases to a few percent of the CO_2 density in the atmosphere.

The main optical emission from hot air is due to the two electronic states of nitrogen, the second positive N_2, $C\,^3\Pi_u$-$B\,^3\Pi_g$, and the first negative system of the ion N_2^+, $B\,^2\Sigma_u^+$-$X\,^2\Sigma_g^+$. The optical emission due to these bands is re-

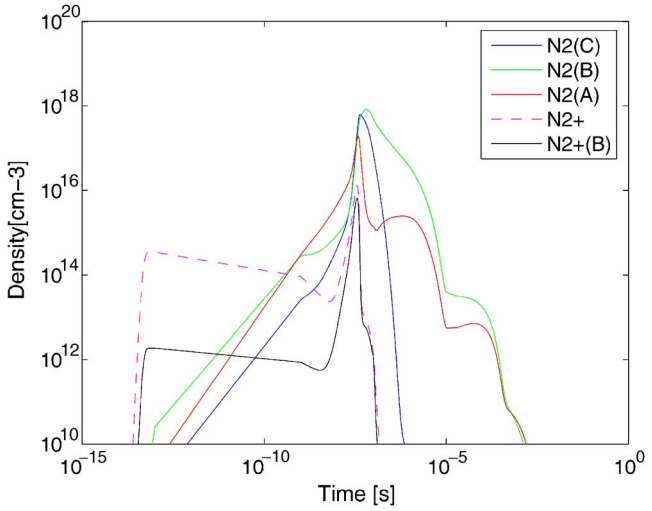

FIG. 8. (Color online) Temporal evolution of the number densities of the species $N_2(A)$, $N_2(B)$, $N_2(C)$, N_2^+, and N_2^+ (B) for DLP case.

duced due to collisional quenching by a time dependent factor, $1/[1+\tau_R(n_{N_2}k_{q,N_2}+n_{O_2}k_{q,O_2})]$, where τ_R is the respective radiative lifetime, k_{q,N_2} and k_{q,O_2} are the rate constants for collisions with nitrogen and oxygen molecules,[17] and n_{N_2}, n_{O_2} are the time dependent populations of nitrogen and oxygen molecules. The infrared emission in the first positive band of the nitrogen molecule, $B\,^3\Pi_g$-$A\,^3\Sigma_u^+$, is strongly quenched out at the high gas pressure. The number densities of the levels involved in the above transition as a function of time are shown in Fig. 8.

It is important to emphasize that the emission is a nonlinear process, and the emission intensity in the above bands depends nonlinearly on the intensity of the CO_2 laser. This is clearly shown in Fig. 9, which shows the intensity in the above molecular bands as a function of the intensity of the CO_2 laser. It can be seen that the plasma emission is substantially increased in comparison with irradiation with the USPL only, indicating that a flare at a remote position in the atmosphere can be generated. Specifically, the emission at 4.26 μm increase by two orders of magnitude. The optical

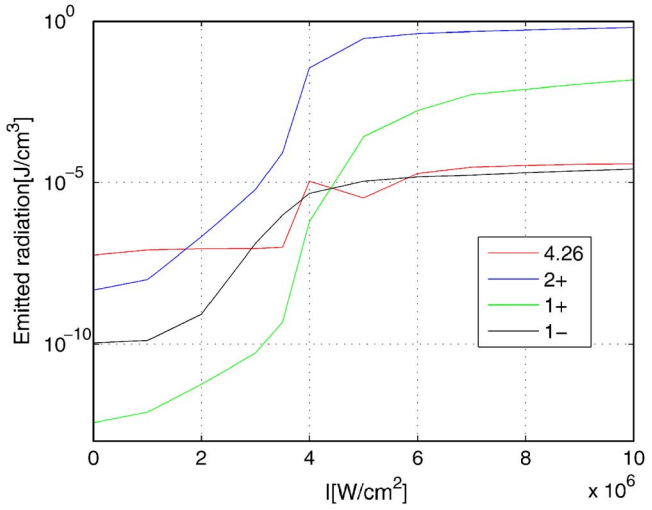

FIG. 9. (Color online) The emission in several molecular bands as a function of the CO_2 laser intensity

emission in the second positive band of N_2 is estimated to be higher by two orders of magnitude. The relative increase in the emission in the first positive band as a function of the CO_2 laser intensity is the highest. For intensity above 5×10^6 W/cm^2, the emission in this band is obtained to be larger by about three orders of magnitude than the emission in the first negative band of N_2, usually considered in laser produced plasmas in air. The time of cooling of the hot channel to ambient temperature is increased from 1.4 ms to 18 ms at intensity of 10^7 W/cm^2. Of special importance is the fact that the ratio of intensities of the above molecular bands strongly depends upon the intensity of the CO_2 laser. Thus, by varying the latter, one can control the spectrum of the radiation source.

IV. A POTENTIAL LABORATORY PROOF-OF-PRINCIPLE EXPERIMENT

The above analysis suggests that an energetic radiation source can be generated at a remote location in the atmosphere by using a combination of a high intensity short laser pulse and a low intensity long duration laser pulse. A potential proof-of-principle laboratory experiment can be performed using a pulsed Ti:sapphire laser system at 798 nm with power exceeding by a factor of 10 or more the filamentation threshold for air (~5 GW); for example, a 100 f Ti:sapphire system with energy of few tens of millijoules and 10 Hz or more repetition rate would suffice. A lens configuration ($f\sim1-5$ m) can be used to create the filamentation pattern at short distances in the laboratory. This pattern can then be illuminated using a commercial pulsed CO_2 laser that can deliver several hundreds of millijoules in about 100 ns. The CO_2 laser intensity can be varied using a focusing lens and the radiation emitted by the plasma filament in the second positive band of N_2 (around 0.3 μm), and the first negative band of N_2^+ (around 0.4 μm) can be measured using a simple spectrometer coupled, for example, to an ICCD (intensified charged coupled device).

ACKNOWLEDGMENTS

Useful discussions with Dr. T. Wallace and Dr. P. Sprangle are highly appreciated. The Work at the University of Maryland was supported by BAE Systems-AT.

[1] A. Couairon and A. Mysyrowicz, Phys. Rep. **441**, 47 (2007).
[2] P. Sprangle, J. R. Penano, and B. Hafizi, Phys. Rev. E **66**, 046418 (2002).
[3] M. Rodriguez, R. Bourayou, G. Mejean, J. Kasparian, J. Yu, E. Salmon, A. Scholz, B. Stecklum, J. Eisloffel, U. Laux, A. P. Hatzes, R. Sauerbrey, and L. Woste, Phys. Rev. E **69**, 036607 (2004).
[4] G. Fibich, S. Eisenmann, B. Ilan, Y. Erlich, M. Fraenkel, Z. Henis, A. I. Gaeta, and A. Zigler, Opt. Express **13**, 5897 (2005).
[5] Z. Q. Hao, J. Zhang, Y. T. Li, X. Lu, X. H. Yuan, Z. Y. Zheng, Z. H. Wang, W. J. Ling, and Z. Y. Wei, Appl. Phys. B: Lasers Opt. **80**, 627 (2005).
[6] P. Rambo, J. Schwartz, and J.-C. Diels, J. Opt. A, Pure Appl. Opt. **3**, 146 (2001).
[7] Ya. B. Zeldovich and Yi. P. Raizer, *Physics of Shock Waves and High-Temperature Hydrodynamic Phenomena* (Academic, New York, 1966), Vol. I.
[8] A. V. Gurevich, N. D. Borisov, and G. M. Milikh, *Physics of Microwave Discharges Artificially Ionized Regions of the Atmosphere* (Gordon and Breach Science, Amsterdam, 1997).
[9] F. Vidal, D. Comtois, C.-Y. Chien, A. Desparois, B. La Fontaine, T. W. Johnston, J.-C. Kieffer, and H. P. Mercure, IEEE Trans. Plasma Sci. **28**,

418 (2000).
[10]A. Kossyi, Y. Kostinsky, A. A. Matveyev, and V. P. Silakov, Plasma Sources Sci. Technol. **1**, 207 (1992).
[11]G. Milikh, J. A. Valdiva, and K. Papadopoulos, J. Atmos. Sol.-Terr. Phys. **60**, 907 (1998).
[12]G. Milikh, D. A. Usikov, and J. A. Valdivia, J. Atmos. Sol.-Terr. Phys. **60**, 875 (1998).
[13]A. Talebpour, S. Petit, and S. L. Chin, Opt. Commun. **171**, 285 (1999).
[14]F. Martin, R. Mawassi, F. Vidal, I. Gallimberti, D. Comtois, H. Pepin, J. C. Kieffer, and H. P. Mercure, Appl. Spectrosc. **56**, 1444 (2002).
[15]D. R. Keefer, B. B. Henriksen, and W. F. Braerman, J. Appl. Phys. **46**, 1080 (1975).
[16]R. J. Nordstrom, Appl. Spectrosc. **49**, 1490 (1995).
[17]S. V. Pancheshnyi, S. M. Starikovskaya, and A. Yu. Starikovskii, Plasma Phys. Rep. **23**, 616 (1997).